View metadata, citation and similar papers at core.ac.uk

brought to you by CORE

provided by Missouri University of Science and Technology (Missouri S&T): Scholars' Mine

Missouri University of Science and Technology

Scholars' Mine

International Specialty Conference on Cold-Formed Steel Structures

(1971) - 1st International Specialty Conference on Cold-Formed Steel Structures

Aug 20th, 12:00 AM

Shock Loading of Thin Compression Elements

Charles G. Culver

Richard Van Tassel

Follow this and additional works at: https://scholarsmine.mst.edu/isccss

Part of the Structural Engineering Commons

Recommended Citation

Culver, Charles G. and Tassel, Richard Van, "Shock Loading of Thin Compression Elements" (1971). *International Specialty Conference on Cold-Formed Steel Structures*. 1.
https://scholarsmine.mst.edu/isccss/1iccfss/1iccfss-session3/1

This Article - Conference proceedings is brought to you for free and open access by Scholars' Mine. It has been accepted for inclusion in International Specialty Conference on Cold-Formed Steel Structures by an authorized administrator of Scholars' Mine. This work is protected by U. S. Copyright Law. Unauthorized use including reproduction for redistribution requires the permission of the copyright holder. For more information, please contact scholarsmine@mst.edu.

SHOCK LOADING OF THIN COMPRESSION ELEMENTS

By Charles G. Culver[1], and Richard Van Tassel[2], Assoc. Members, ASCE

INTRODUCTION

The existing specification (11)[3] governing the design of cold-formed steel structural members used for load-carrying purposes in buildings is based on static loading considerations. The extensive theoretical and experimental investigations which form the basis for these specifications have provided a thorough understanding of the behavior of these members subjected to static loads.

The use of cold-formed members is not restricted to building construction, however, and under various environmental conditions these members are subjected to time-dependent or dynamic loads (8). Containers fabricated from cold-formed elements subject to shock or impact loading during transportation or collision problems involving vehicles which utilize cold-formed load carrying members are two examples of this type of environmental condition.

A considerable number of theoretical and experimental investigations dealing with structural response due to time-dependent loading have been conducted. This information ranges from the analysis and design of structures subjected to blast or earthquake loads to the response of simple beams subjected to transverse impact. Several comprehensive reviews and literature surveys of these studies are available. These existing studies deal primarily with structural elements commonly encountered in heavy construction such as hot-rolled WF beams and columns. Due to fundamental differences between the behavior of cold-formed members and that of the heavier hot-rolled sections, a direct application of this information to problems involving cold-formed members is not always possible.

The purpose of this paper is to present the results of the first phase of a research project directed toward developing a fundamental understanding of the response of cold-formed members subjected to time-dependent loading. The scope of this investigation is limited to structural elements subjected to rapidly applied short duration force, displacement, velocity or acceleration pulses. Loadings of this type are generally referred to as mechanical shock.

MATHEMATICAL MODEL

The basic concept underlying the design of cold-formed members involves the utilization of the postbuckling strength of the compression elements which comprise the cross sections of these members. This postbuckling behavior and the associated concept of "effective width" introduce nonlinearities in the response of cold-formed sections and necessitate an iterative type trial and error design procedure for static loading. In order to understand the behavior of cold-formed members subjected to shock loading, it is therefore necessary to first establish the postbuckling behavior of thin compression elements subjected to in-plane shock loading.

The postbuckling behavior of thin plates subjected to static edge loads has been studied by several investigators. A summary of the principal results in this area has been presented by Jombock and Clark (6). Only a limited amount of work has been done on the behavior of thin plates subjected to dynamic forces applied in the middle-plane of the plate. Zizicas (15) applied small deflection plate theory to problems of this type to investigate the relationship between transverse vibrations and overall plate instability. Other studies in this area (3, 10) have been concerned with the dynamic stability of plates subjected to periodically varying forces applied in the middle plane. To the writer's knowledge, studies of the postbuckling response of thin plates subjected to transient edge loading have not been conducted.

The problem considered in this paper is illustrated in Fig. 1. The thin compression element shown in Fig. 1 is subjected to a time varying load P(t) applied in the middle plane. It is assumed that the load is applied through a rigid loading bar and does not vary across the width of the element. The initial deflection of the middle surface prior to application of the load is denoted by $w_o(x,y)$. The element is assumed to be simply supported with respect to deflections normal to the middle plane. Two conditions of restraint with respect to in-plane displacements along the longitudinal unloaded edges will be considered. In the first case the longitudinal edges remain straight but are free to move laterally. For Case 2, lateral displacement of the longitudinal edges is completely restrained.

The mathematical model used in this study was the same as that developed by Bolotin (3) for dynamic stability studies of plates subjected to periodic edge loading. Bolotin's model was extended, however, to include initial imperfections, $w_o(x,y)$, by using the strain-displacement relations derived by Hu, et. al. (5). Using the following large deflection plate equation

$$\nabla^4(w-w_o) = \frac{1}{D}\left[N_x \frac{\partial^2 w}{\partial x^2} + 2\, N_{xy} \frac{\partial^2 w}{\partial x \partial y} + N_y \frac{\partial^2 w}{\partial y^2}\right] \tag{1}$$

and the differential equations for the in-plane displacements, u, v, the following nonlinear differential equation for the transverse deflections was derived using Galerkin's method

$$\frac{d^2 S(\tau)}{d\tau^2} + S(\tau)\left[1 - \frac{P(\tau)}{P^*}\right] + \left[S^2(\tau) - 2S_o\, S(\tau)\right]\left[S(\tau) + S_o\right]\gamma - S_o \frac{P(\tau)}{P^*} = 0 \tag{2}$$

In applying Galerkin's method, the initial transverse deflection, $w_o(x,y)$, and the total deflection, $w(x,y)$, including deflection w_o, which satisfy the boundary conditions for simply supported edges were taken as

$$w_o = f_o \sin\frac{\pi x}{a} \sin\frac{\pi y}{b} \tag{3a}$$

$$w = f(t) \sin\frac{\pi x}{a} \sin\frac{\pi y}{b} \tag{3b}$$

The initial and final deflection amplitudes and the time variable in Eq. 2 were nondimensionalized as

$$S_o = \frac{f_o}{h}, \quad S = \frac{(f-f_o)}{h} \tag{4a}$$

$$\tau = \frac{t}{t_n} = \omega_n t \tag{4b}$$

The form of Eq. 2 for both conditions of restraint with respect to in-plane displacements, Case 1, Case 2 is the same. The parameters used to nondimensionalize the results were as follows

Case 1

---

[1]Associate Professor of Civil Engineering, Carnegie-Mellon University, Pittsburgh, Pennsylvania.

[2]First Lieutenant, U. S. Army, Corps of Engineers; formerly graduate student, Carnegie-Mellon University, Pittsburgh, Pennsylvania.

[3]Numerals in parentheses refer to corresponding items in Appendix I - References.

$$p^* = \frac{\pi^2 Da}{b^2}\left(1 + \frac{b^2}{a^2}\right)^2 \tag{5a}$$

$$\gamma = \frac{3(1-\nu^2)}{4}\,\frac{\left(1 + \frac{a^4}{b^4}\right)}{\left(1 + \frac{a^2}{b^2}\right)^2} \tag{5b}$$

<u>Case 2</u>

$$p^* = \frac{\pi^2 Da}{b^2}\,\frac{\left(1 + \frac{b^2}{a^2}\right)^2}{\left(1 + \nu\frac{b^2}{a^2}\right)} \tag{6a}$$

$$\gamma = \frac{3(1-\nu^2)}{4}\,\frac{\left(3 + \frac{a^4}{a^4}\right)}{\left(1 + \frac{a^2}{b^2}\right)^2} \tag{6b}$$

In deriving Eq. 2, the inertia terms associated with in-plane displacements, stress wave propagation, were neglected. For a square plate, the ratio of the time required for the stress wave to traverse the plate once to the natural period is equal to $0.8/(a/h)$. For $a/h = 60$ this ratio is approximately 0.013. Since the time duration of the shock loads of interest in this study are usually longer than 0.1 times the natural period, the above assumption is reasonable.

Since Eq. 2 is a nonlinear differential equation with variable coefficients, a closed form solution would be difficult if not impossible to obtain. This equation was therefore solved on a CDC G-20 digital computer using a special program (12) written in ALGOL. This computer program is based on analog computer concepts and utilizes numerical integration operations to solve the differential equation. An iterative prediction correction scheme which is required to converge to a specified error criterion is used to simulate the feedback principle inherent in analog computers.

Three pulse shapes or time variation of the transient edge loading were considered as shown in Fig. 1. These forcing functions have been used in previous dynamic response studies (1, 3, 4) and in certain cases they approximately simulate the shock loading induced in practical situations.

After solving Eq. 2 for the time function $S(\tau)$, the transverse deflections may be found using Eq. 3. The longitudinal strain and stress in the middle plane may then be evaluated using the strain-displacement and stress-strain equations (3).

Before discussing the general results obtained from this mathematical model, it is of interest to compare certain specific results obtained in this study with those of earlier studies. Comparison with both static and dynamic studies will be made.

As mentioned previously, the concept of effective width introduced by von Kármán has been used when considering the elastic postbuckling strength of plates. Eq. 2 is valid for the case of static loading if the first term, $d^2S(\tau)/d\tau^2$, is set equal to zero. Note that if this is done and the initial deflection parameter, S_o, is also set equal to zero, Bleich's expression (2) for the postbuckling deflections is obtained. Defining effective width as

$$\bar{\sigma}_{max}\, a_{eff} = (N_y)_{max}/h = \sigma a = (P/ah)\, a \tag{7}$$

solving Eq. 2, substituting the result into the stress-strain relations to obtain $(N_y)_{max}$ and using Eq. 7 gives the following relationship for a square plate

$$\frac{a_{eff}}{h} = \frac{1}{\left\{1/(a/h) + (\pi^2/8)(E/\sigma)\left[1/(a/h)\right]^3 (S^2 + 2S_oS)\right\}} \tag{8}$$

The relationship for determining the effective width in Eq. 8 is the same for both conditions of longitudinal edge restraint, cases 1 and 2. The

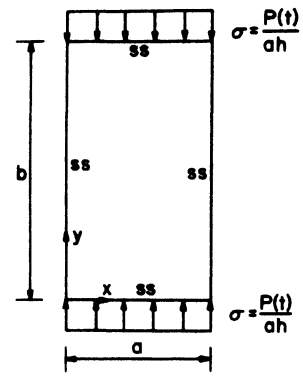

CASE 1-Longitudinal Edges Free to Move Laterally (Mean Edge Stress=0)
CASE 2-Longitudinal Edges Cannot Move Laterally (Mean Edge Strain=0)

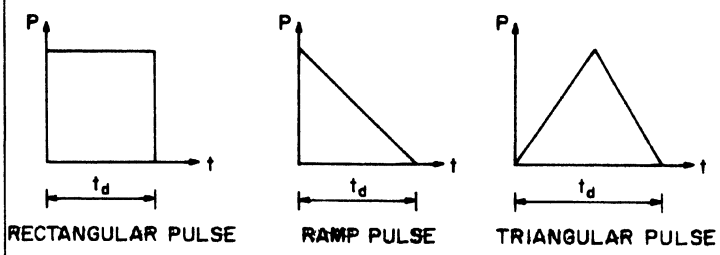

FIGURE 1 - Compression Element Subjected to Time-Dependent Loading

actual resulting effective widths for the two cases differ, however, since the nondimensional deflection, S, obtained from Eq. 2 for the two cases is different.

Based on an extensive series of static beam tests, Winter developed the following formula for effective width

$$\frac{a_{eff}}{h} = 1.9\sqrt{\frac{E}{\bar{\sigma}_{max}}}\left[1 - 0.415\left(\frac{1}{a/h}\right)\sqrt{\frac{E}{\bar{\sigma}_{max}}}\right] \tag{9}$$

Note that the design equation used for the effective width of stiffened compression elements (11) may be obtained from Eq. 9 by introducing an appropriate factor of safety of 1.67.

A comparison of the effective width obtained from Eqs. 8, 9 for the two cases of longitudinal edge restraint as well as two values of initial imperfections, is presented in Table 1 in nondimensional form, (a_{eff}/a). The values of S used in Eq. 8 to obtain these results are presented elsewhere (13). The edge stress used in Eqs. 8, 9 is specified in terms of the buckling stress for the square plate.

Referring to Table 1, the effective widths for cases 1 and 2 decrease as the initial imperfections increase. Also for lower values of stress, $\sigma/\sigma_{cr} \leq 1.0$, the effective width for a particular value of initial imperfections is less for case 2 than for case 1. As the stress increases, however, this tendency is reversed. The difference between case 1 and 2 results from the Poisson ratio effect associated with the longitudinal edge restraint.

Comparison of the results obtained from Eq. 9 with those from Eq. 8 indicate that Eq. 9 predicts a smaller effective width in most cases. This result is not surprising since Eq. 9 represents a conservative or lower bound approximation to test data. The percent difference between these effective widths is a function of stress level. The maximum percent difference between the results in Table 1 for Eqs. 8, 9 is 10%.

The actual amount of initial imperfections, S_o, present in the elements which comprise the cross section of cold-formed beam specimens is difficult

TABLE 1 - COMPARISON OF EFFECTIVE WIDTH

$\frac{\sigma}{\sigma_{cr}}$ (1)	$(a_{eff}/a)_{Eq\ 9}$ (2)	$(a_{eff}/a)_{case\ 1}$ $S_o = 0.1$ (3)	Difference, as a percentage (4)	$S_o = 0.2$ (5)	Difference, as a percentage (6)	$(a_{eff}/a)_{case\ 2}$ $S_o = 0.1$ (7)	Difference, as a percentage (8)	$S_o = 0.2$ (9)	Difference, as a percentage (10)
0.5	0.978	0.977	0	0.943	-3.7	0.959	-2.0	0.910	-7.5
1.0	0.782	0.867	9.8	0.808	2.5	0.820	4.6	0.789	0
1.5	0.672	0.727	7.5	0.690	2.6	0.730	7.9	0.706	4.8
2.0	0.599	0.640	6.4	0.632	5.2	0.666	9.9	0.645	7.1

$$\text{Difference, as a percentage} = \frac{\text{Eq 8} - \text{Eq 9}}{\text{Eq 8}}$$

$$\sigma_{cr} = \frac{4\pi^2 E}{12(1-\nu^2)(\frac{a}{h})^2}, \qquad E = 29{,}500 \text{ Ksi}, \qquad \nu = 0.3$$

to establish. Although "out of flatness" tolerances are specified for the sheet material to be used to cold form these specimens, similar tolerances are not specified for the finished cross section. In addition, the compression elements in beam sections are not simply supported as assumed but are rotationally restrained by the other elements of the cross section. Based on the results presented in Table 1, however, it appears that the mathematical model reasonably represents the behavior of compression elements in cold-formed sections. The validity of these results for the case of dynamic loading and the influence of initial imperfections and rotational edge restraint should be experimentally verified in a manner similar to that used in developing Eq. 9 for static loading.

The dynamic response of an element subjected to a long duration rectangular pulse, $S_o = 0.1$, $\beta' = 1.6$, obtained by solving Eq. 2 is shown in Fig. 2. The results are presented in nondimensional form for several values of the magnitude of the applied load. The dynamic response according to linear small deflection theory (15) is also shown. The dimensionless parameter used for the ordinate in Fig. 2 is the same as that used by Zizicas.

Note that both small deflection and large deflection theory predict the same initial response. As time increases, however, small deflection theory overestimates the response. The difference between the linear and nonlinear response is a function of the load magnitude, $\alpha' = P/P^*$. As α' increases the difference between the response using the linear and nonlinear theory also increases. For loads greater than the buckling load, $\alpha' > 1$, the dynamic deflections according to small deflection theory increase indefinitely with time. Due to the inclusion of the nonlinear terms in the strain-displacement equations, large deflection theory, however, predicts finite deflections.

The influence of the load function or pulse shape for case 1 on the transverse deflections is shown in Fig. 3. The response is plotted as a function of time for the three pulse shapes considered in Fig. 1. Equal values of the maximum load were used for each pulse and the load durations were chosen such that the impulse or area under the load-time curve was the same for each pulse; i.e. with $\alpha' = 2$ and impulse = 1.274. $\beta' = 0.637$ for the rectangular pulse and $\beta' = 1.274$ for the ramp and triangular pulses.

The response curves in Fig. 3 indicate that the rectangular pulse causes the largest deflection. Over the first few time units, the response due to the ramp pulse and rectangular pulse are nearly equal. After some time, however, the two curves show considerable difference. Initially the triangular pulse has negligible response compared to the other pulses. This is due to the low initial magnitude of the forcing function in the equation of motion, Eq. 2. After approximately five time units, the deflection due to the triangular pulse exceeds that of the ramp pulse, which has started decreasing. Upon removal of the load, the deflections are due to free vibration. Note that the free vibration is unsymmetrical with respect to the τ axis. This behavior occurs because of the nonlinear terms in the equation of motion. Also, the periods of free vibration are inversely related to the amplitude of vibration.

Previous studies have indicated that the following parameters affect the dynamic response, of simple structures subjected to shock loading:

1. Time variation of load (pulse shape)
2. Load duration
3. Load magnitude

Based on the behavior of compression elements subjected to static loading (6), the following additional parameters should be included for the specimens in in this investigation:

4. Initial imperfections
5. Boundary conditions

The influence of these five parameters on the transverse deflection at an antinode point, point of maximum deflection, and the mid-plane strain at the edge of the element is shown in Figs. 4 through 9 in nondimensional form for a square plate. Note that the appropriate value of P^*, Eqs. 5a, 6a, was used for cases 1 and 2 to nondimensionalize the load. These results were obtained by dividing the maximum response, deflection or strain, produced by the dynamic load by the corresponding value produced by a statically applied load equal to the maximum dynamic load. This dimensionless ratio may be referred to as an impact factor, amplification factor or dynamic load factor.

Referring to Figs. 4, 5 and 6, the influence of the time variation or pulse shape of the externally applied load is apparent. On the basis of the maximum impact factor, the rectangular pulse is obviously the most severe loading case. The ramp pulse approaches this case as the time duration, β', increases. Note in Fig. 6 that as the time duration of the triangular pulse increases, the impact factor approaches unity and the maximum response approaches that produced by static loading.

The influence of the pulse shape discussed above is similar to that obtained in previous studies (1) of the response of a linear single mass oscillator. The nonlinearities in the present problem apparently do not affect this influence. Note that the use of Eq. 3b in the analysis essentially reduces the system under consideration to a single degree of freedom.

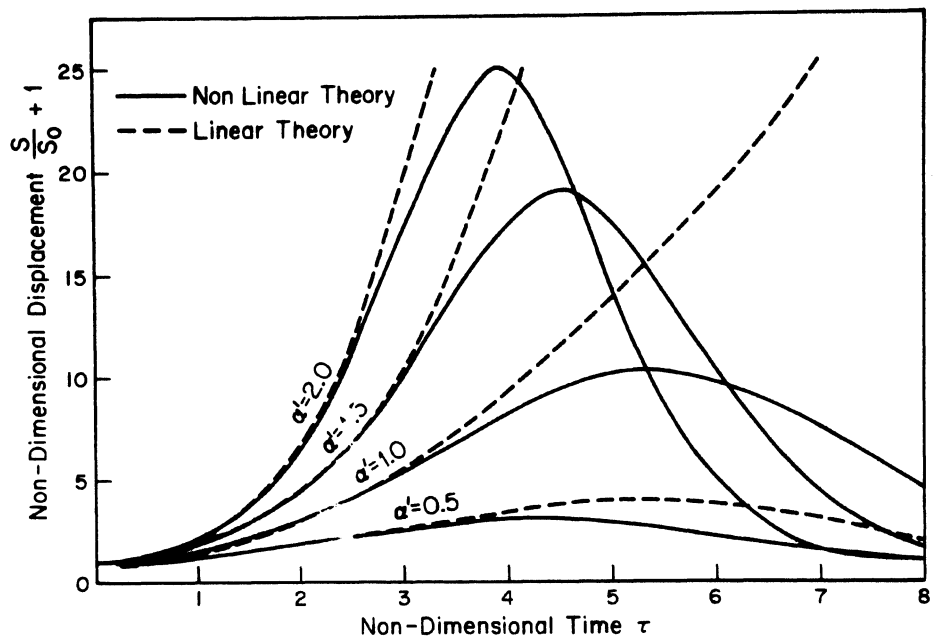

FIGURE 2 - Comparison of Linear and Nonlinear Response - Case 1

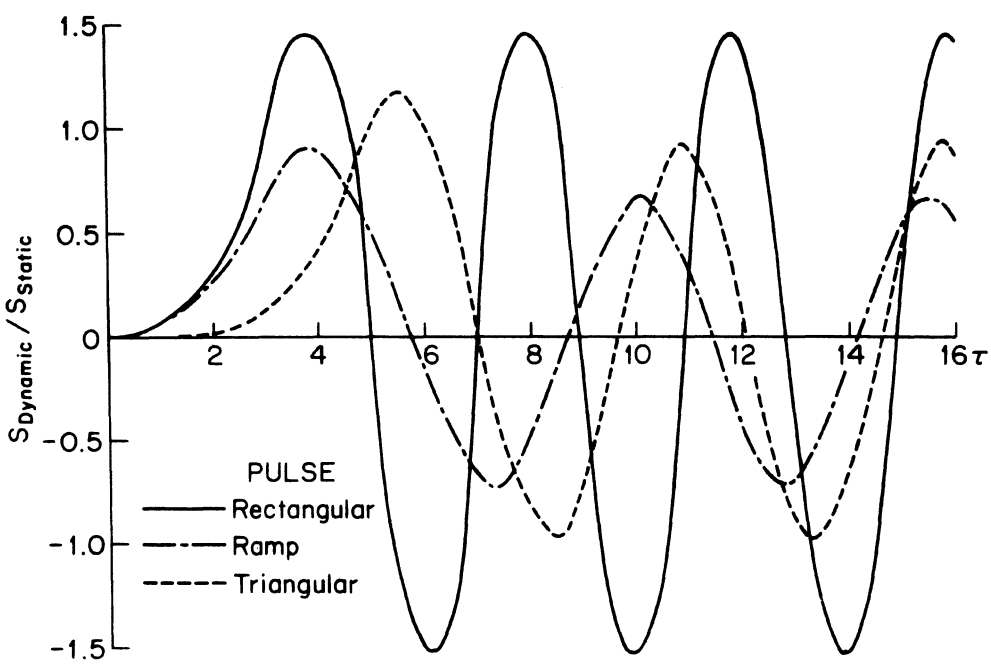

FIGURE 3 - Influence of Load Function on Response - Case 1

The influence of load duration on the maximum response is also similar to that obtained from the analysis of linear systems. For a very short load duration, the dynamic effect is less than the static effect. For extremely short load durations, the effects of stress wave propagation should be considered. As the load duration increases, the dynamic effect is pronounced. The time durations required for the impact curves to reach their maximum values, however, are longer than the time durations for the linear single mass oscillator (1). This behavior is in agreement with previous studies of the dynamic response of nonlinear systems (1, 4, 9).

The irregularity or bump in the curves for the rectangular pulse in Fig. 4 which occurs as the impact factors reach their maximum value is related to the nonlinearity of the equations of motion. Over this range of time durations, the maximum transverse deflections occurred in the first cycle just after removal of the load pulse as the element began to vibrate freely. The second bump in Fig. 4 for $S_0 = 0.2$ and $\beta' = 1.4$ was also caused by this same effect. The range of time durations for which this phenomenon occurred was small and, in general, the maximum response occurred during the time interval β' associated with application of the load pulse. This phenomenon also occurred for the other pulse shapes considered but the associated time duration did not correspond to that for which the maximum impact factor occurred. This effect is not apparent for the other pulse shapes since the resulting irregularities in the impact factor curves were small.

The influence of initial imperfections on the dynamic response may be evaluated by comparing the two graphs presented for each pulse shape and load magnitude in Figs. 4, 5, 6. Referring to Fig. 4, for example, not that an increase in initial imperfections from $S_0 = 0.1$ to $S_0 = 0.2$ tends to shift the

response curve to the left.

The influence of the boundary conditions on the response of the plate may be evaluated by comparing the curves for case 1 and 2 in Figs. 4, 5, 6. Referring to Fig. 4, for example, this influence depends upon the duration of the applied load. For short duration loads, the increased edge restraint considered in case 2 tends to increase the impact factor. As the load duration increases, however, the influence of this restraint becomes less significant and the

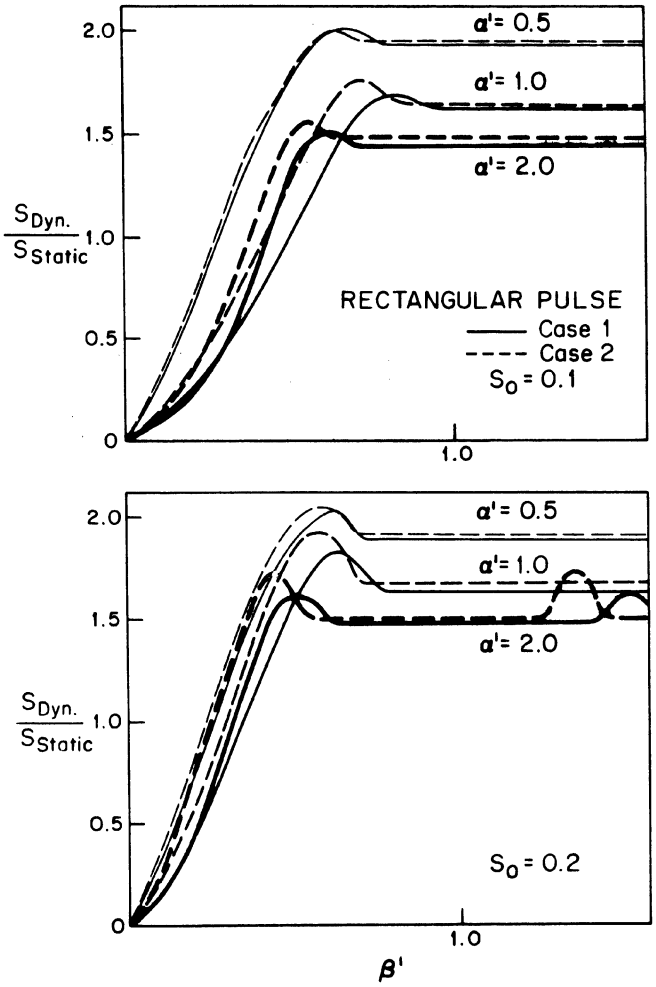

FIGURE 4 - Rectangular Pulse Impact Factors - Deflection

response for cases 1 and 2 are essentially the same. Thus for long duration dynamic loads, the influence of the in-plane boundary conditions is the same as that for static loading: i.e.,

$$\left(\frac{S_{dyn}}{S_{stat}}\right)_{Case\ 1} \approx \left(\frac{S_{dyn}}{S_{stat}}\right)_{Case\ 2} \longrightarrow \frac{\left(S_{dyn}\right)_{Case\ 1}}{\left(S_{dyn}\right)_{Case\ 2}} = \frac{\left(S_{stat}\right)_{Case\ 1}}{\left(S_{stat}\right)_{Case\ 2}}$$

The influence of the boundary conditions also depends upon the shape of the load pulse. For example, the differences between cases 1 and 2 for the triangular pulse are less than those for the rectangular pulse for short duration loads.

The various parameters mentioned above influence the mid-plane edge strains and transverse deflections in a similar manner. Note however, that the maximum impact factors for edge strains are less than for transverse deflections. This is particularly true when the applied loads are less than the buckling load, $\alpha' < 1$. For example, referring to Fig. 9, the impact factor for the triangular pulse with $\alpha' = 0.5$ is only slightly greater than 1.0 regardless of the load duration, whereas the maximum impact factor for deflections in Fig. 6 is 1.34.

The dynamic effect of short duration loading is also different for the edge strains and transverse deflections. As the load duration decreases the dynamic

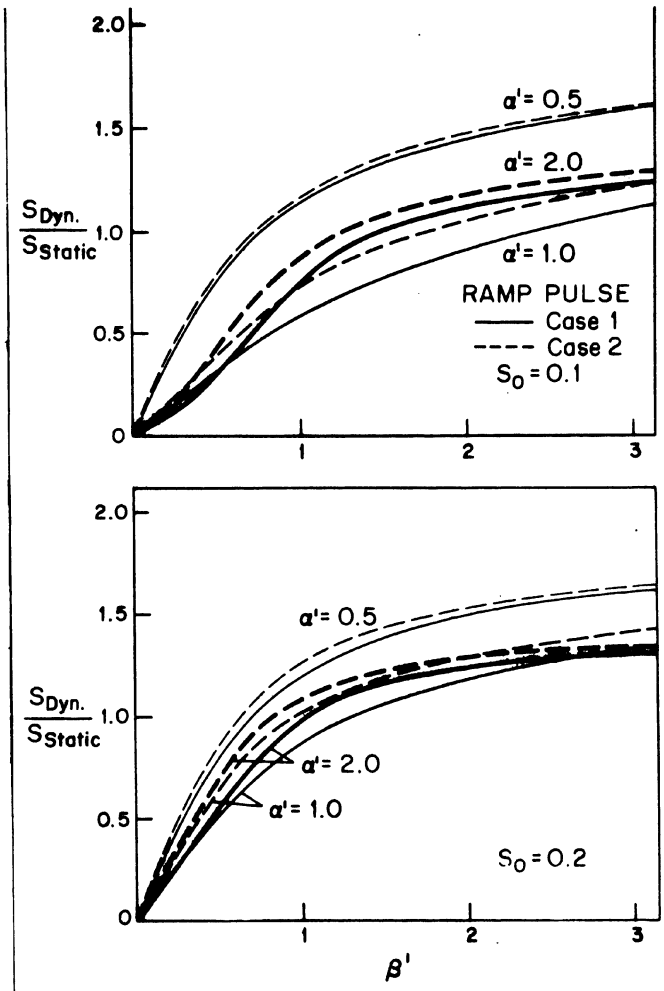

FIGURE 5 - Ramp Pulse Impact Factors - Deflection

deflections decrease and are substantially less than those produced under static loading. Theoretically for an infinitely short load duration the transverse deflections and the corresponding impact factors approach zero. The impact factors for the strains, however, do not approach zero and the curves level off as the load duration decreases. Since stress wave propagation was neglected the strain in the plate has a finite value for $\beta' > 0$. The curves however, have a discontinuity at $\beta' = 0$, $\varepsilon_{dyn}/\varepsilon_{static} = 0$, since obviously no load is applied to the plate.

Note that the edge strain impact factors for cases 1 and 2 are very nearly equal over the entire range of load durations and the influence of the in-plane boundary conditions on strains is the same as that for static loading.

The accuracy of the above results were checked by using a two term expansion for the deflection in Eq. 3b. The resulting response spectra were the same. The maximum difference between the impact factors was 9% with the two term expansion giving lower values as expected.

Based on the preceding discussion and the results presented in Fig. 4 through 9, the following conclusions may be drawn:

1. The influence of the time variation of the applied loads on the impact factors for deflections is qualitatively similar to that obtained for linear single mass oscillators.
2. The magnitude of the impact factor for edge strains decreases for short duration loads and increases for longer duration loads, as the maximum applied load increases.
3. In general, the influence of the in-plane boundary conditions on the

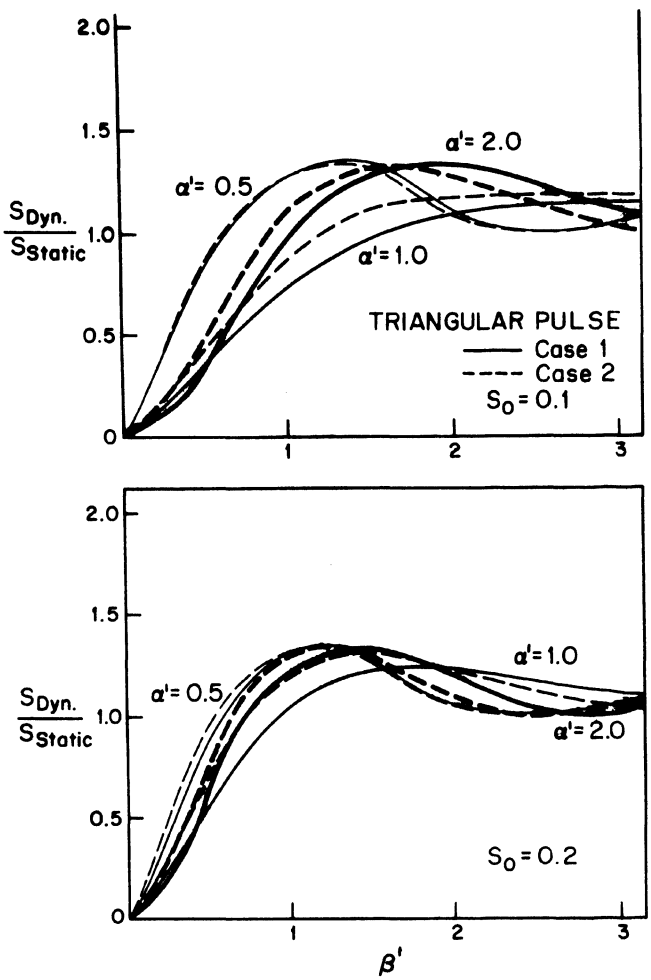

FIGURE 6 - Triangular Pulse Impact Factors - Deflection

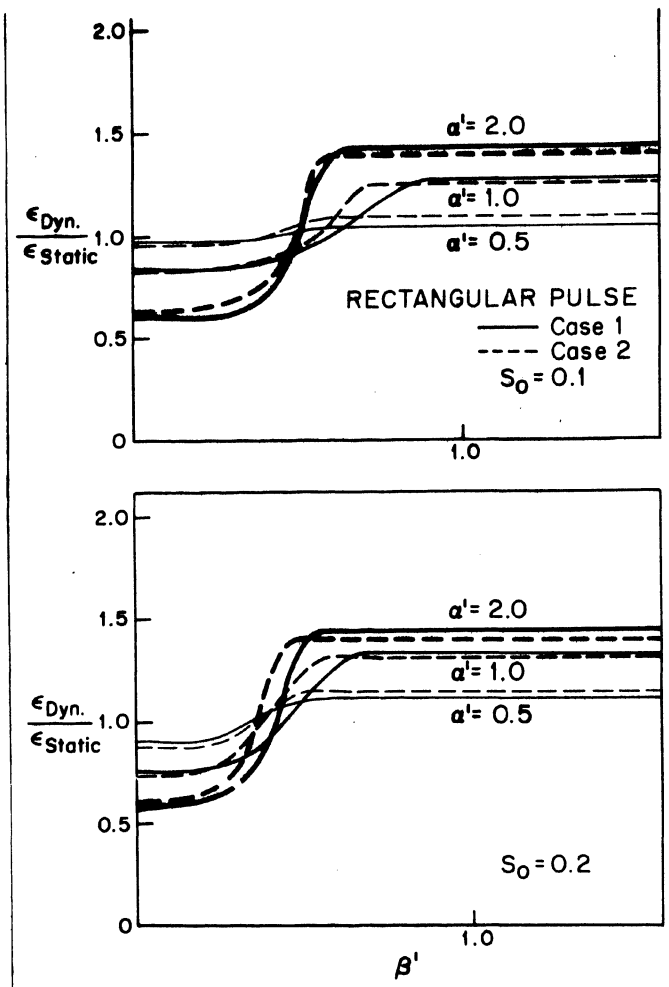

FIGURE 7 - Rectangular Pulse Impact Factors - Edge Strain

mid-plane edge strains is the same as for static loading.

APPLICATION OF RESULTS

The results presented above dealt with individual compression elements. In practical applications where impact or shock loading is of interest, however, the structures involved consist of load carrying members cold-formed to shape from flat sheet or plate. In order to extend these results to practical cases it is necessary therefore, to compare the dynamic behavior of individual elements to that of cold-formed structural members such as beams and columns.

A qualitative extension of these results is given in Fig. 10. The ratio of the maximum mid-plane dynamic edge strain to the maximum static edge strain is plotted as a function of β' for the triangular load pulse. Note that this relationship was obtained by idealizing the response curve in Fig. 9 for $\alpha' = 2.0$, $S_0 = 0.1$ by four straight lines. Using this ratio as a modification factor for the edge stress in Eq. 9 in computing the effective width, a "dynamic effective width" was calculated. The ratio of the dynamic effective width to the static value is also shown in Fig. 10. These results represent the minimum value of effective width which would occur during the dynamic response of the elements. For short duration loads, $\beta' \leq 1.3$ the dynamic effective width is greater than the static value. As the time duration of the load increases, $\beta' > 1.3$, the dynamic value is less than the static value. For extremely long duration loads, this value obviously approaches unity. For an 8" square 16 gage plate, the value of $\beta' = 3.2$ at which the static and dynamic effective widths are approximately equal corresponds to a load duration of 0.018 seconds. Note that the above results would change for different pulse shapes, load magnitudes, initial imperfections and boundary conditions.

For the case of static loading, the primary difference between the behavior of an individual element in edge compression and the compression flange of a beam specimen or the elements comprising the cross section of an axially loaded column is the rotational restraint or boundary conditions provided by the adjoining elements of the cross section. The influence of this rotational restraint is obviously also important for the case of shock loading. In addition, the influence of cold-forming on the material properties in the vicinity of the juncture of two plates is also important (7).

A direct analytical extension of the results presented herein to the case of cold-formed beams and columns subjected to shock loading would be extremely complicated. A combined analytical and experimental approach was therefore initiated in order to establish the behavior of these members (14). The qualitative results established from the parameter study in the preceding section are being utilized in these further studies. For example, in the case of a cold-formed beam subjected to shock loading, the internal force in the compression flange varies with time due to the overall beam vibrations. Based on the results of the dynamic response of linear elastic beams (1) the most severe shock loading, maximum amplification of bending moment, due to inertia effects associated with the beam vibrations would occur for a duration of the external load pulse equal to the natural period of the beam. For the nonlinear beam, however, considering the compression flange of the beam as a rotationally restrained compression element loaded into the postbuckling range, results presented herein indicate that the time variation, period, of the internal moment with respect to the natural period of the compression flange, i.e. β', is important. Since the natural

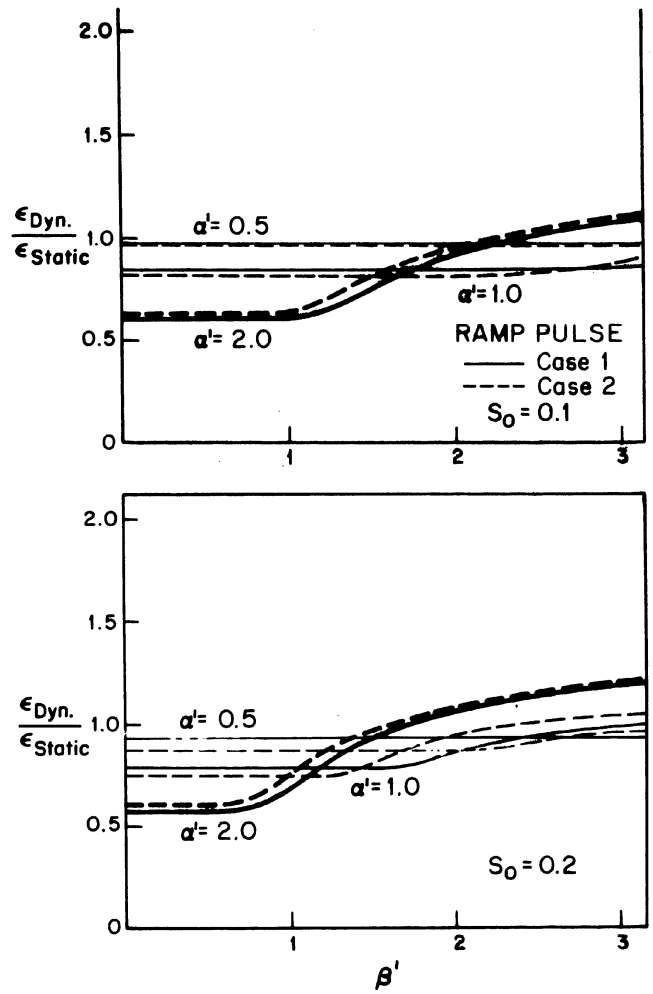

FIGURE 8 - Ramp Pulse Impact Factors - Edge Strain

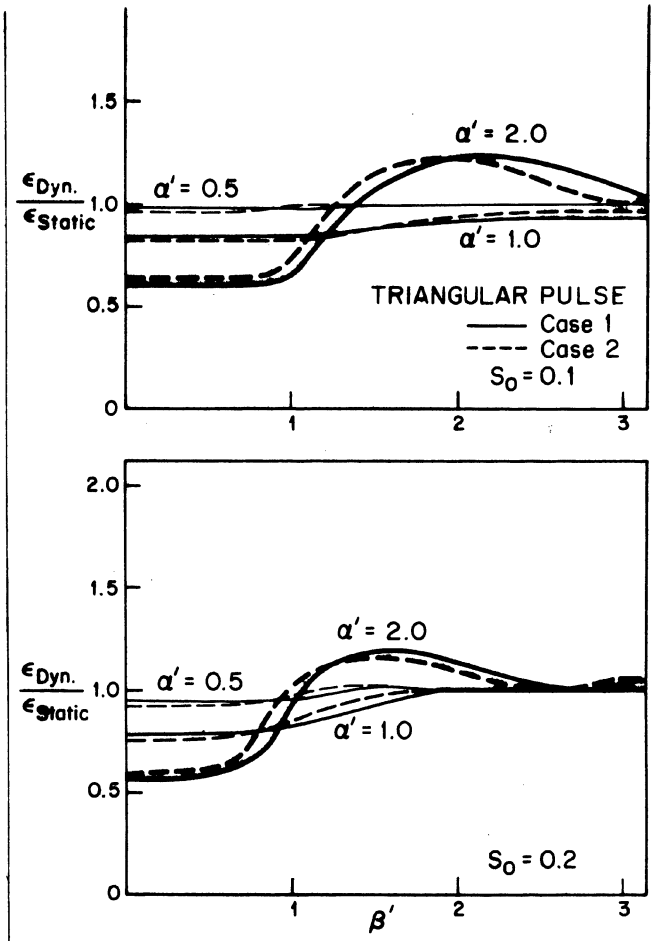

FIGURE 9 - Triangular Pulse Impact Factors - Edge Strain

period of the compression flange is usually considerably different from the natural period of the overall beam, both the beam response and the response of the elements comprising the beam cross section may have to be considered in order to establish design criteria related to the severity of shock loading. Note that load durations β' of the order of magnitude of those in Fig. 10 would be considerably less than the natural period of the beam for practical cold-formed beams. Considerations of this nature were used in developing the experimental program mentioned above.

For the case of axially loaded columns subjected to shock loading it may be possible to use the preceding results to develop modified form factors, Q , (11) for cold-formed column sections. Studies of this type are also underway.

The analytical results and the applications mentioned above were based on the assumption of linear elastic behavior of the material. It was therefore implicitly assumed that initial yielding at the edges of the element constitutes failure. A similar assumption was used to formulate static design specifications for cold-formed members and plastic design procedures are not permitted. For the case of shock loading, however, the behavior of these members after failure may be important in certain applications. For example, in designing collapsible type structures with high energy absorption capabilities (8), the total behavior of the specimen up to complete rupture or tearing of the metal may be important. Therefore, the failure modes of cold-formed members as well as their load-deflection history after the edge strains reach yield should be studied.

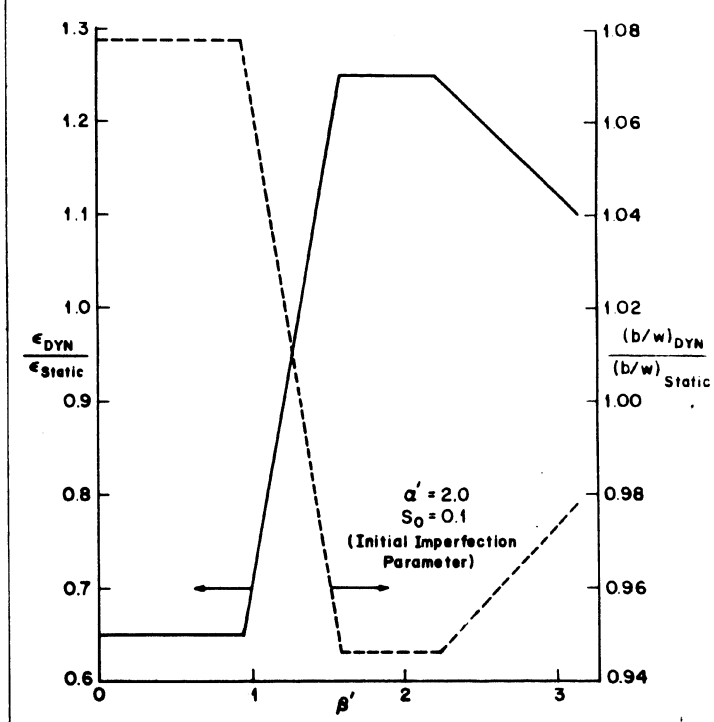

FIGURE 10 - Influence of Dynamic Loading on Effective Width

SUMMARY AND CONCLUSIONS

The nonlinear equations governing the elastic response of thin compression elements loaded into the postbuckling range by dynamic edge loads applied in the middle plane were formulated and solved. Based on a number of cases considered, the relationship between the parameters which affect the dynamic response were evaluated. It is anticipated that the results obtained in this study will be of use in establishing the behavior of cold-formed structural members subjected to shock loading.

ACKNOWLEDGMENTS

The work reported in this paper represents the first phase of a research program on "Light Gage Cold-Formed Steel Structural Elements Subjected to Time-Dependent Loading" sponsored by the American Iron and Steel Institute and conducted in the Department of Civil Engineering of Carnegie-Mellon University, Pittsburgh, Pa. The cooperation of W. G. Kirkland, Vice President, AISI and the members of the AISI Task Group on the Influence of Dynamic Loading on Structural Behavior of Light Gage Steel, R. B. Matlock, Chairman, J. B. Scalzi and C. R. Clauer is gratefully acknowledged.

APPENDIX I - REFERENCES

1. Biggs, J. M., Introduction to Structural Dynamics, McGraw-Hill Book Company, Inc., New York, 1964.
2. Bleich, F., Buckling Strength of Metal Structures McGraw-Hill Book Company, Inc., New York, 1952.
3. Bolotin, V. V., The Dynamic Stability of Elastic Systems, Holden Day, Inc., San Francisco, 1964.
4. Design of Structures to Resist Nuclear Weapons Effects, ASCE, Manual No. 42, 1964 Edition.
5. Hu, P. C., Lundquist, E. E., and Batdorf, S. B.,"Effect of Small Deviations from Flatness on Effective Width and Buckling of Plates in Compression," NACA Technical Note No. 1124, 1946, Washington, D. C.
6. Jombock, J. R. and J. W. Clark, "Postbuckling Behavior of Flat Plates," Transactions, ASCE, Vol. 127, Part II, 1962, pp. 227.
7. Karren, K. W. and Winter, G., "Effects of Cold-Forming on Light-Gage Steel Members" Journal of the Structural Division, ASCE, Vol. 93, ST 1, Proc. Paper 5113, February 1967, pp. 433-469.
8. Pugsley, A., "The Crumpling of Tubular Structures Under Impact Conditions," The Institute of Locomotive Engineers, Symposium Proceedings, Paper No. 4, London, May 27, 1960.
9. Schultz, A. B., "Nonlinear Response of a Beam to Shock Pulse," Journal of the Franklin Institute, Nov., 1963, pp. 385-393.
10. Somerset, J. H.,"Transition Mechanisms Attendant to Large Amplitude Parametric Vibrations of Rectangular Plates," Journal of Engineering for Industry, ASME, Vol. 89, 1967, pp. 619.
11. Specification for the Design of Cold-Formed Steel Structural Members, American Iron and Steel Institute, 1968.
12. Strauss, J. C. and W. L. Gilbert, "A Programming System for the Simulation of Combined Analog Digital Systems," Third Edition, Carnegie Institute of Technology, 1964.
13. Van Tassel, R., "Large Deflection Theory for Plates Subjected to Dynamic Edge Loading," University Microfilms, Ann Arbor, Mich., 1968.
14. Zanoni E. A., "Nonlinear Analysis of Light Gage Cold-Formed Beams Subjected to Shock Loading," University Microfilms, Ann Arbor, Mich., 1969.
15. Zizicas, G. A., "Dynamic Buckling of Thin Elastic Plates," Journal of Applied Mechanics, Transactions, ASME, October 1952, pp. 1257-1268.

APPENDIX II - NOTATION

The following notation is used in this paper:

a, b = lengths of sides of rectangular element, in.;

a_{eff} = effective width used to account for nonuniform distribution of longitudinal stress, in.;

$D = \frac{Eh^3}{12(1-\nu^2)}$ = flexural rigidity, lb. in.;

E = modulus elasticity, lb. in.$^{-2}$;

f = amplitude of transverse deflection, in.;

f_o = amplitude of initial transverse deflection, in.;

h = thickness of element, in.;

N_y = longitudinal force in middle plane per unit length, lb. in.$^{-1}$;

P = external force in middle plane, lbs.;

P^* = Eq. 5a, 6a, lbs;

$S = \frac{f-f_o}{h}$ = nondimensional transverse deflection;

$S_o = \frac{f_o}{h}$ = nondimensional initial transverse deflection;

t = time, sec.;

t_d = time duration of applied load, sec.;

t_n = $1/\omega_n$, sec.;

T = natural period $(2\pi/\omega_n)$, sec.;

u, v = in-plane displacements in x and y directions averaged over thickness, in.;

$w(x,y)$ = total transverse deflection of a point in middle plane (including initial imperfections), in.;

$w_o(x,y)$ = initial transverse deflection, in.;

x,y = rectangular coordinates;

$\alpha' = \frac{P}{P^*}$ = nondimensional load;

γ = Eqs. 5b, 6b;

$\tau = \frac{t}{t_n}$ = nondimensional time;

$\beta' = \frac{t_d}{T}$ = nondimensional load duration;

ω_n = lowest natural frequency of transverse vibration, rad. sec.$^{-1}$;

σ = stress, lb. in.$^{-2}$;

$\bar{\sigma}_{max}$ = maximum longitudinal edge stress in middle plane, lb. in.$^{-2}$;

ν = Poisson's ratio; and

$\nabla^4 = \frac{\partial^4}{\partial x^4} + \frac{2\partial^4}{\partial x^2 \partial y^2} + \frac{\partial^4}{\partial y^4}$.